---

**Article:**
Torres, O, Mercado Tena, N, Murray, B orcid.org/0000-0002-6493-1547 et al. (1 more author) (2017) Novel starch based emulsion gels and emulsion microgel particles: Design, structure and rheology. Carbohydrate Polymers, 178. pp. 86-94. ISSN 0144-8617

https://doi.org/10.1016/j.carbpol.2017.09.027

---

# Novel starch based emulsion gels and emulsion microgel particles: Design, structure and rheology

**Ophelie Torres[1], Nidia Mercado Tena[1], Brent Murray[1] and Anwesha Sarkar [1] ***

[1]Food Colloids and Processing Group, School of Food Science and Nutrition, University of Leeds, Leeds LS2 9JT, UK

*Corresponding author:

Dr. Anwesha Sarkar

Food Colloids and Processing Group,

School of Food Science and Nutrition, University of Leeds, Leeds LS2 9JT, UK.

E-mail address: A.Sarkar@leeds.ac.uk (A. Sarkar).

Tel.: +44 (0) 113 3432748.

## Abstract

Novel starch-based emulsion microgel particles were designed using a facile top-down shear-induced approach. The emulsion droplets were stabilized using octenyl succinic anhydride (OSA) modified starch and incorporated into heat-treated and sheared native starch gels, forming emulsion gels. Using gelation kinetics and small deformation rheological measurements of sheared native starch gels and emulsion gels, OSA starch-stabilized emulsion droplets were demonstrated to act as "active fillers". By varying native starch concentrations (15-20 wt%) and oil fractions (5-20 wt%), optimal concentrations for the formation of emulsion microgel particles were identified. Microscopy at various length scales (transmission confocal laser scanning and cryo-scanning electron microscopy) and static light scattering measurements revealed emulsion microgel particles of 5-50 μm diameter. These novel emulsion microgel particles created via careful combination of gelatinized native starch and OSA stabilised-emulsion droplets acting as active fillers may find applications in food and personal care industries for delivery of lipophillic molecules.



## Keywords

Emulsion microgel particle; native starch; OSA starch; encapsulation; rheology; active filler


## 1 Introduction

Lipophilic molecules, such as flavourings, essential oils or drugs pose considerable challenges when incorporated into food, pharmaceuticals and other soft matter applications, due to their partial or complete water insolubility. Because of this and their susceptibility to oxidation, most of these compounds are difficult to deliver pre- and post-consumption (McClements, 2015). A wide range of emulsion-based approaches have been developed to encapsulate oil-soluble molecules, such as conventional emulsions, nanoemulsions, double emulsions, emulsion gels, etc, (Zhang, Zhang, Chen, Tong & McClements, 2015).

Emulsion microgel particles are a relatively new class of soft solids vehicle that has not been explored as widely. The particles have a similar structure to emulsion gels, although their physical characteristics and length scales differ. In emulsion microgel particles, emulsion droplets are stabilised by an emulsifier and gelling agent inside a larger (microgel) particle (Torres, Murray & Sarkar, 2016, 2017). In other words, several emulsion droplets are encapsulated together within a soft solid shell. The soft solid shell around the oil droplets has been demonstrated to protect lipophilic compounds against oxidation (Beaulieu, Savoie, Paquin & Subirade, 2002). The microgel particle itself can be dispersed in a controlled manner in an aqueous media. Additionally, microgel particles allow swelling or de-swelling as a function of environmental conditions, tuning their size and/or physicochemical properties, enabling the protection and possible release of lipophilic active compounds in a range of soft material applications (Ballauff & Lu, 2007; Wei, Li & Ngai, 2016). Hence, it is important to design such emulsion microgel particles using biocompatible polymers, such as starch, which is the second most abundant biopolymer in nature.

Native starch is widely used in commercial applications and its versatility as a gelling agent is well-recognized (Teyssandier, Cassagnau, Gérard & Mignard, 2011; Zhang et al., 2013). Drastic changes in the microstructure and viscoelastic properties of starch gels can be generated by shearing during gelatinization. Previous studies have shown that shear breaks down the swollen granules into smaller fragments producing a more viscous and translucent gel. These smaller fragments have been suggested to be responsible for decreasing the rigidity by acting as inactive fillers in the amylose gel matrix (Lu, Duh, Lin & Chang, 2008; Svegmark & Hermansson, 1991).

The incorporation of solubilized modified starch into non-sheared gelatinized native starch has also been reported to affect the viscoelasticity and retrogradation properties of native starch gels (Thirathumthavorn and Charoenrein, 2006, Tukomane and Varavinit, 2008). On the other

hand, starch modified with octenyl succinic anhydride (OSA) has been widely demonstrated to stabilize oil-in-water emulsions, via the addition of hydrophobic groups (OSA) to the starch molecules (Zhang et al., 2015, Nilsson and Bergenståhl, 2006, Tesch et al., 2002). The incorporation of hydrophobic groups in OSA starch molecules has been suggested to retard hydrogen bonding between amylose molecules in the native starch dispersions, hindering the gelation process (Thirathumthavorn and Charoenrein, 2006, Tukomane and Varavinit, 2008, Bao et al., 2003). Aggregation of OSA groups has also been shown to allow the formation of a network via hydrophobic interactions between adjacent OSA starch chains (Ortega-Ojeda et al., 2005, Thirathumthavorn and Charoenrein, 2006, Tukomane and Varavinit, 2008). Nevertheless, no studies have been performed to understand the interaction between OSA starch at the oil-water interface and sheared gelatinized native starch. It is critical to understand how OSA starch-stabilized emulsion droplets would bind to a sheared starch matrix within an emulsion gel and how this would influence processing of this starch-based emulsion gel into emulsion microgel particles via a top-down approach i.e., controlled shearing.

To our knowledge, there is only one study in the literature describing production of starch-based microgel particles, however involving protein coated oil droplets (Malone and Appelqvist, 2003). In this study, starch granules were dispersed into a low oil fraction ($\leq$ 10wt%) sodium caseinate-stabilised oil-in-water emulsion, which was then heat treated to allow the starch to gelatinize, followed by moulding into gel particles of 3 mm of diameter. It is worth recognizing that thermodynamic incompatibility between the protein and the starch at the oil/water interface might result in uncontrolled release behaviour as well as instability of the particles over time if the oil fraction was increased above 10 wt%. The large particle size ($> 45\,\mu$m) might also limit food applications due to possible impact on sensory perception (Torres, Murray & Sarkar, 2016). An alternative would be to explore designing OSA starch-stabilized emulsion droplets embedded into a sheared starch matrix. In addition, it would be

crucial to understand how gel stiffness and emulsion droplet binding to the starch matrix would affect the ability to break up such a system into emulsion microgel particles via a controlled shearing process (top-down approach).

Therefore, the objectives of this study were firstly to understand the interactions between OSA starch-stabilized emulsions and gelatinized sheared native starch and secondly to design starch-based emulsion microgel particles using a controlled shearing process. As a control, the interactions between solubilized OSA starch and sheared native starch were also studied using small deformation rheology. It is hypothesised that the OSA-stabilised emulsion droplets would strongly bind to the sheared native starch gel as an "active filler" and this should enable break up of this emulsion gel into microgel particles without any oil leakage.

## 2 Material and Methods

### 2.1 Materials

Wheat native starch was purchased from Sigma-Aldrich (Gillingham, UK). Commercial OSA starch refined from waxy maize starch was used. Sunflower oil was obtained from Morrisons (UK) supermarket. All dispersions were prepared with Milli-Q water having a resistivity of 18.2 MΩ·cm at 25 °C (Milli-Q apparatus, Millipore, Bedford, UK). All other chemicals were of analytical grade and purchased from Sigma-Aldrich unless otherwise specified.

### 2.2 Determination of amylose content of native wheat starch and waxy OSA starch

The amylose content was determined using a spectrophotometer (6715 UV/Vis. Spectrophotometer, Jenway, Keison Ltd, UK) following the method developed by Kaufman, Wilson, Bean, Herald and Shi (2015).

The amylose standard curve was prepared using different ratios of pure amylose from potato and pure amylopectin from corn starch purchased from Sigma-Aldrich (Dorset, UK).

The regression equation was determined from the standard curve using the absorbance difference between 620 and 510 nm. The amylose content of the different starch sample was then calculated using eq (1):

$$Amylose\ \% = \frac{(Abs\ 620 - Abs\ 510) - y\ intercept\ of\ regression}{slope\ of\ regression} \quad (1)$$

### 2.3 Preparation of stock modified starch stabilized emulsions

The OSA starch at different concentrations (1.7, 3.4 and 6.7 wt%) was dissolved in Milli-Q water and gently stirred (500 rpm) for 2 h using a magnetic stirrer.

Sunflower oil was subsequently mixed with the OSA starch dispersion at ambient temperature. The ratio of the lipid phase to aqueous phase in the emulsion was 40:60 (w/w), with a final OSA starch concentration of 1, 2 or 4 wt%. These oil-aqueous phase mixtures were pre-emulsified with a high speed rotor-stator mixer (Silverson, L5M-A, UK) at 8,000 rpm for 5 min for 1 and 2 wt% OSA starch or 10 minutes for 4 wt% OSA starch. The pre-emulsions were further homogenized in a laboratory scale two-stage valve high pressure homogenizer at 250/50 bar using two passes (Panda Plus, GEA Niro Soave, Parma, Italy). The emulsion samples were stored at 4 °C for 24 h for further analysis.

### 2.4 Particle size analysis

The particle size distribution of the emulsion droplets and emulsion microgel particles was measured via a Malvern Mastersizer 3000E hydro, (Malvern Instruments, Worcestershire, UK). Sizing of the emulsion oil droplets was conducted based on a relative refractive index (RI) of 1.097 (i.e., the ratio of the RI of sunflower oil (1.46) to that of the aqueous phase (1.33)). Sizing of the emulsion microgel particles was conducted based on a relative RI of 1.150 (i.e., the ratio of the RI of the particle (1.5) to that of the aqueous phase at (1.33)). For comparison

of particle size distributions, $d_{32} = (\sum n_i d_i^3 / \sum n_i d_i^2)$ and $d_{43} = (\sum n_i d_i^4 / \sum n_i d_i^3)$ were calculated.

### 2.5 Preparation of mixed gels and emulsion gels

Native starch gels were formed by dispersing native wheat starch in MilliQ water and heating at 80 °C for 40 minutes in a water bath. Simultaneously, shear treatment was continuously applied for two minutes with three minutes interval using a hand blender (Hand blender, XB986B, 170W, Argos, UK).

Emulsion gels containing different concentrations of native starch (15 or 20 wt%), OSA starch (0.5, 1, 1.5 or 2 wt%) and oil fractions (5, 10, 15, 20 wt%) were prepared by mixing native starch gels with 40 wt% oil-in-water emulsion stabilized by 4 wt% OSA starch at different ratios. Table 1 summarizes the different initial and final concentrations of native starch and OSA starch as well as oil fraction.

Table 1. Initial and final concentrations of native starch and 40 wt% oil-in-water emulsion stabilised by 4 wt% OSA starch as well as mixing ratios for the formation of the different emulsion gels.

| **Native starch gel** | **Oil-in-water Emulsion** | | **Native starch gel : Emulsion Ratio** | **Native starch gel** | **Oil-in-water Emulsion** | |
|---|---|---|---|---|---|---|
| Initial [NS] (wt%) | Initial [oil] (wt%) | Initial [OSA] (wt%) | | Final [NS] (wt%) | Final [oil] (wt%) | Final [OSA] (wt%) |
| 17.2 | 40 | 4 | 87.5:12.5 | 15 | 5 | 0.5 |
| 20 | | | 75:25 | | 10 | 1 |
| 24 | | | 62.5:37.5 | | 15 | 1.5 |
| 30 | | | 50:50 | | 20 | 2 |
| 22.9 | 40 | 4 | 87.5:12.5 | 20 | 5 | 0.5 |
| 26.7 | | | 75:25 | | 10 | 1 |
| 32 | | | 62.5:37.5 | | 15 | 1.5 |
| 40 | | | 50:50 | | 20 | 2 |

For comparison purposes, OSA starch dispersions without any oil droplets was also mixed with native starch using the same ratios as for the emulsion gels, forming mixed OSA starch-native starch gels.

The different ratios of OSA starch dispersion or emulsion were first heat treated to 80 °C before being vigorously mixed with the sheared starch gel at 80 °C, allowing the formation of starch mixed gels and emulsion gels, respectively.

### 2.6 Small deformation rheology

Small deformation viscoelasticity of the different gels was investigated under dynamic oscillatory shear rheometry using a Kinexus ultra rheometer (Malvern Instruments Ltd. Worcestershire, UK). A cone-and-plate geometry system (40 mm, model: CP4/40 SS017SS) was used for all measurements. About 0.5 mL of gel was placed onto the sample plate and sealed with a thin layer of the 350 cst silicone oil to prevent evaporation.

The elastic modulus (G') and viscous modulus (G'') were measured firstly while conducting a strain sweep between 0.01 and 100 % strain, at 1 Hz and 25 °C, to determine the linear viscoelastic region. A frequency sweep was also conducted between 0.6 to 63 rad $s^{-1}$ at 0.5 % strain and 25 °C to determine the complex viscosity (η*) of the different gels. The third test performed on the different gels was temperature and time sweep, carried out in the linear viscoelastic region (0.5 % strain) and 1 Hz. The sample plate was preheated to 80 ºC before the addition of the samples. The G' and G'' were measured during two different temperature changes: (a) cooling at 4 ºC $min^{-1}$ from 80 ºC to 25 ºC and (b) holding at 25 ºC for 66 minutes. The limiting deformation value ($\dot{\gamma}_L$) of the different gels was arbitrarily chosen as the point where the elastic modulus decreased by 20% from the first value of the modulus measured at 0.1 % strain.

## 2.7 Preparation of emulsion microgel particles

Emulsion microgel particles were produced using a top-down approach as illustrated in Figure 1. The sheared native starch gels or emulsion gels were refrigerated at 4 °C for three hours. The refrigerated emulsion gels were then passed twice through a laboratory scale two-stage valve high pressure homogenizer at 250/50 bar (Panda Plus, GEA Niro Soave, Parma, Italy). The resulting particles were collected in a beaker and immediately diluted with Milli-Q water and stirred for 30 min at 150 rpm to limit particle aggregation.

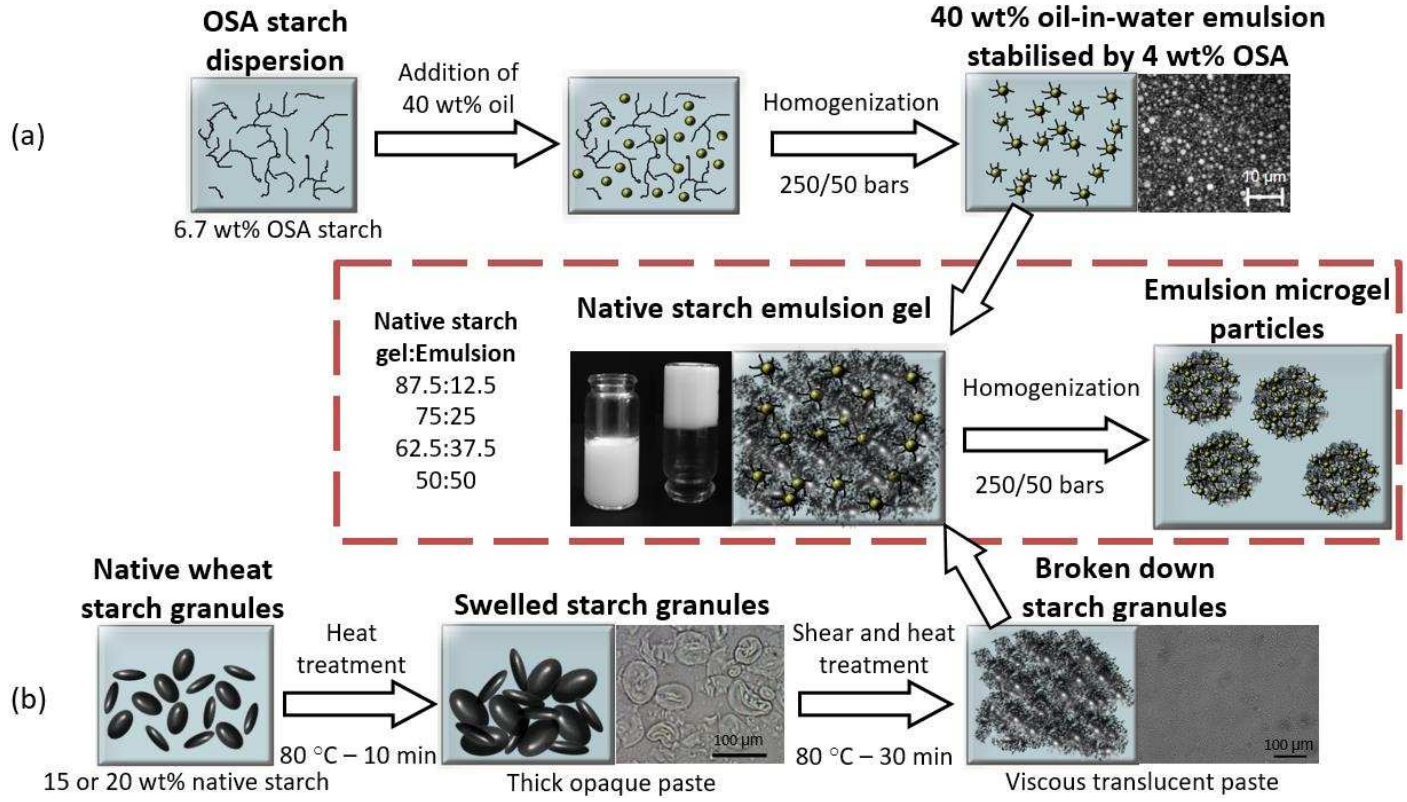


Figure 1. Schematic diagram and corresponding micrographs of the formation of OSA starch-stabilised emulsion (a), sheared native starch gel (b) and native starch emulsion gel and emulsion microgel particles (indicated within dashed box).

## 2.8 Microscopy

All emulsions, emulsion gels and emulsions microgel particles (50 $\mu$L) were imaged via optical microscopy (Nikon, SMZ-2T, Japan), confocal laser scanning microscopy (CLSM) and cryo-

scanning electron microscopy (cryo-SEM). A Zeiss LSM 700 confocal microscope (Carl Zeiss MicroImaging GmbH, Jena, Germany) with a 40× magnification lens was used. About 10 $\mu$L of Nile Red (1 mg $mL^{-1}$ in dimethyl sulfoxide, 1:100 v/v) was used to stain oil (argon laser with an excitation line at 488 nm), 10 $\mu$L of Nile Blue (0.1 mg $mL^{-1}$ in Milli-Q water, 1:100 v/v) was used to stain native starch (HeNe with an excitation line at 639 nm) and 10 $\mu$L of 1% Methylene Blue was used to stained OSA starch (Ar laser with an excitation line at 639 nm).

A cryo-scanning electron microscope (FEI Quanta 200F FEG ESEM, Japan), equipped with a Quorum PolarPrep 2000 cryo-system was also used to study the structural features of the emulsion microgel particles. A drop of emulsion microgel particles dispersion (10-20 $\mu$L) was placed on rivets mounted on a cryo-SEM stub. These were then frozen in liquid nitrogen slush and then transferred into the PP2000 preparation chamber. The frozen samples were fractured with a blade and carefully etched at -95 °C for 4 min, followed by coating with platinum (5 nm). The samples were then transferred into the cryo-SEM observation chamber for imaging at 5 kV.

### 2.9 Statistical analysis

Data was obtained in triplicate and mean and standard deviation were calculated. Significant differences between samples were determined by one-way ANOVA and multiple comparison test with Tukey's adjustment was performed using SPSS software (IBM, SPSS statistics, version 24) and the level of confidence was 95%.

## 3 Results and Discussion

### 3.1 Effect of the addition of OSA starch on native wheat starch gels

The first set of control experiments were carried out with OSA starch added to native starch without the addition of any emulsion droplets. This sets the scene to understand the interaction between dispersed OSA starch and native starch. Figure 2 shows the elastic (G') and viscous (G'') modulus of the different gels as a function of time and temperature.

All samples can be considered as gels from time 0 s since G' >> G'' and G' remained relatively constant throughout the whole frequency range (0.6 to 60 rad $s^{-1}$) (Supplementary file S1). The gels had similar rheological behaviour irrespective of the concentrations of native starch (15 or 20 wt%) and OSA starch (0 to 2 wt%) used. During the cooling stage, G' increased by over 70% and during the holding stage, G' further increased by approximately 30%. This significant increase in G' can be attributed to the reorganization and association of colloidal- and molecularly- dispersed amylose and amylopectin (Singh, Singh, Kaur, Singh Sodhi & Singh Gill, 2003; Teyssandier, Cassagnau, Gérard & Mignard, 2011).

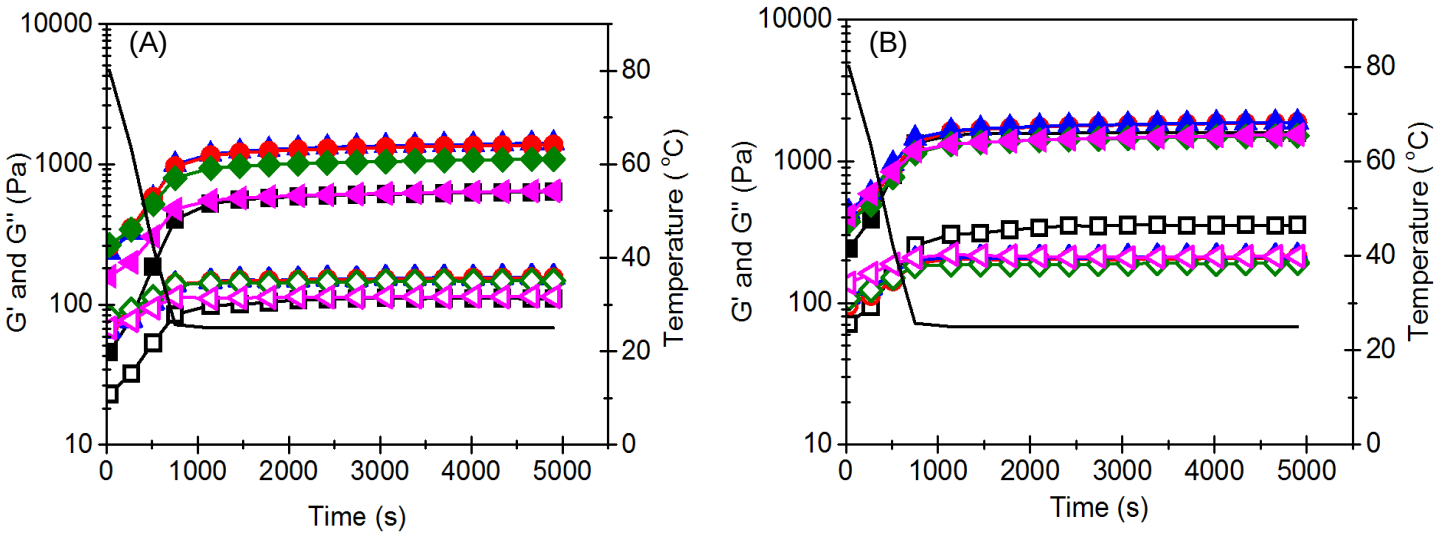


Figure 2. Elastic modulus (G', filled symbols) and viscous modulus (G'', empty symbols) as a function of time and temperature (full black line) of 15 wt% native starch gel (A) and 20 wt% native starch gel (B) prepared with different OSA starch concentrations (0 wt%, ■; 0.5 wt%, ●; 1 wt%, ▲; 1.5 wt%, ♦; 2 wt%, ◄) at 1 Hz and 0.5 % strain.

As expected, the concentration of native wheat starch affected the initial and final elastic modulus of the gels significantly ($p < 0.05$) (Figure 2). For instance, the G' increased by almost one order of magnitude on increasing the native starch concentration by 5 wt% (0.046 ±0.006 kPa for 15 wt% starch, 0.24 ±0.034 kPa for 20 wt% starch). Amylose is the main starch molecule responsible for forming the three-dimensional network (via hydrogen bonding) between the starch chains during gel formation (Miles, Morris, Orford & Ring, 1985; Wang, Li, Copeland, Niu & Wang, 2015). In this study, the amylose content of the native wheat starch and commercial waxy OSA starch were measured to be 18.7% and 0.17%, respectively, in accordance with previous studies (Singh, Singh, Kaur, Singh Sodhi & Singh Gill, 2003). Increasing the concentration of native starch by 5 wt% would therefore increase the amylose content by a factor of 1/4 in the final gel, which explains the significantly higher G' values (Rosalina & Bhattacharya, 2002).

The addition of OSA starch (0.5 to 2 wt%) to 20 wt% sheared native starch gels did not affect the initial and final G' of the gels significantly ($p > 0.05$) (Figure 2B). On the other hand, the addition of OSA starch (0.5 to 2 wt%) to 15 wt% sheared native starch gels significantly increased the initial strength of the gels by over 70% (from 0.046 kPa to 0.2 kPa), respectively (Figure 2A, see supplementary file S2 for statistical analysis). Over time, however, only 0.5 and 1 wt% OSA starch significantly increased the final G' of 15 wt% native starch, by approximately 50%.

Previous studies have demonstrated that high amounts of OSA starch (i.e. minimum ratio of 20:80 by weight, OSA starch:native starch) added to non-sheared native starch affected the retrogradation phenomenon of the gels (Ortega-Ojeda, Larsson & Eliasson, 2005; Tukomane & Varavinit, 2008). The retrogradation process of amylose and amylopectin was found to be retarded due to the substitution of OSA groups on the amylopectin, hindering the hydrogen bonding and re-association between starch molecules via steric hindrance (Bao,

277 Xing, Phillips & Corke, 2003; Thirathumthavorn & Charoenrein, 2006). Additionally, the
278 viscosity and elastic modulus of mixed gels were found to increase significantly. These effects
279 were attributed to the ability of OSA starch to form hydrophobic interactions with other OSA
280 starch molecules (Bhosale & Singhal, 2007; Krstonošić, Dokić & Milanović, 2011).
281 Hydrophobic bonds between neighbouring OSA groups allowed the formation of a network
282 increasing the elastic modulus of the gels (Ortega-Ojeda, Larsson & Eliasson, 2005; Tukomane
283 & Varavinit, 2008). Hence, the addition of 0.5 to 2 wt% OSA starch to the lower concentration
284 of native starch (15 wt%) affected the gel possibly via the same OSA starch-OSA starch cross-
285 linking mechanism. At the higher concentration of native starch (20 wt%), OSA starch had
286 probably little influence on the gels because the usual hydrogen bonds between native starch
287 molecules were more numerous and dominated the gel strength.

288 Figure 3 demonstrates that the addition of OSA starch (0.5 to 2 wt%) affected the linear
289 viscoelastic region (LVER) and limiting deformation value $\dot{\gamma}_L$ of native starch gels, confirming
290 that addition of hydrophobic groups might have an impact on sheared native starch gel. Native
291 starch gels at both 15 and 20 wt%, without OSA starch, had a similar $\dot{\gamma}_L$ ($p > 0.05$) of 10 and
292 3.2 % strain, respectively. The addition of over 1.5 wt% OSA starch to 15 and 20 wt% native
293 starch gels significantly increased $\dot{\gamma}_L$ to over 20 and 25 % strain ($p < 0.05$), respectively, even
294 though their elastic modulus and complex viscosity was similar to their respective native starch
295 gel without OSA starch (Figure 2A and Supplementary file S1A and B). At higher
296 concentration of OSA starch (≥ 1.5 wt%), a denser network might have been formed due to
297 OSA starch aggregation via hydrophobic interactions, which might have decreased the elastic
298 modulus of the mixed gels but increased their flexibility as well as their LVER (Bhosale &
299 Singhal, 2007; Sweedman, Tizzotti, Schäfer & Gilbert, 2013; Wang, Li, Copeland, Niu &
300 Wang, 2015). These OSA starch aggregates would have possibly allowed the gel network to
301 adsorb the energy applied during shearing and deform rather than fracture, for example

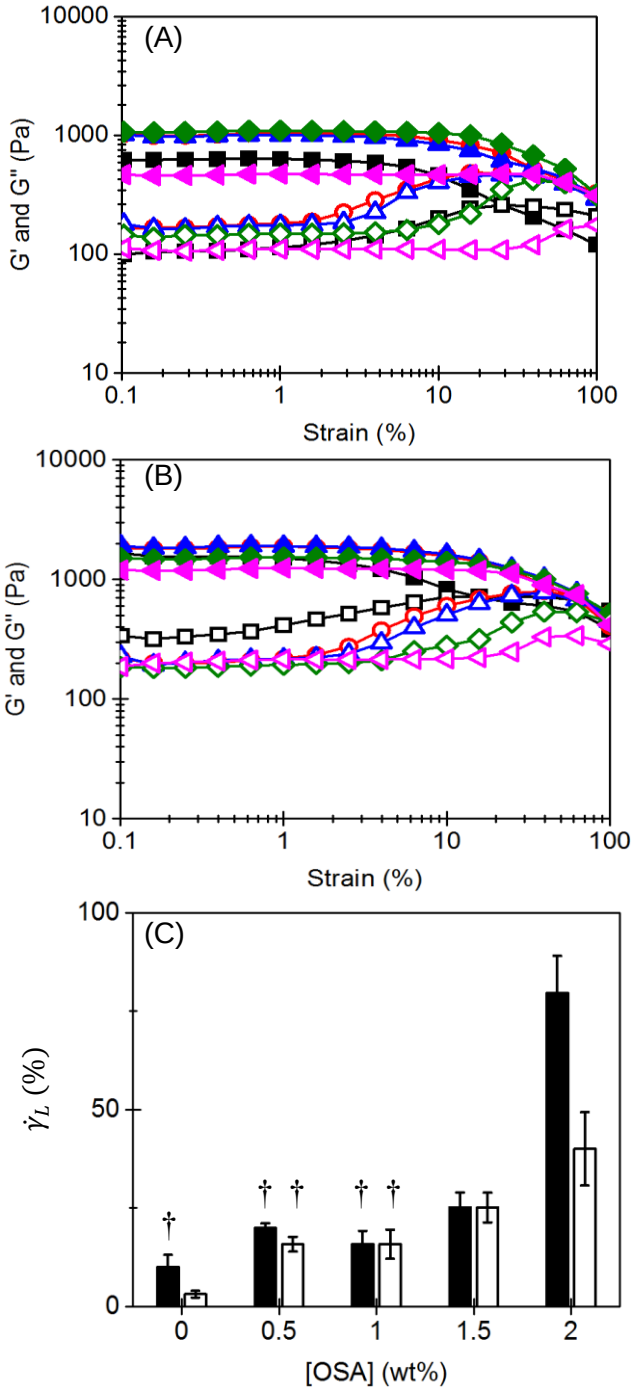


Figure 3. Elastic modulus (G', filled symbols) and viscous modulus (G'', empty symbols) as a function of strain of 15 wt% native starch gel (A) and 20 wt% native starch gel (B) prepared with different OSA starch concentrations (0 wt%, ■; 0.5 wt%, ●; 1 wt%, ▲; 1.5 wt%, ♦; 2 wt%, ◀). The limiting deformation value ($\dot{\gamma}_L$) of native starch gels at 15 wt% (black) and 20 wt% (white) is reported as a function of oil concentration (C), samples with symbol (†) are not significantly different ($p > 0.05$) to native starch gel (15 or 20 wt%) without OSA starch.

(Dickinson, 2012; Torres, Murray & Sarkar, 2017). This reversible decrease in G' is representative of "weak" gel systems, which can undergo a progressive breakdown into smaller clusters with increasing strain. In comparison, "strong" gels under strain break down in an irreversible manner.

### 3.2 Droplet size of OSA-stabilised emulsions

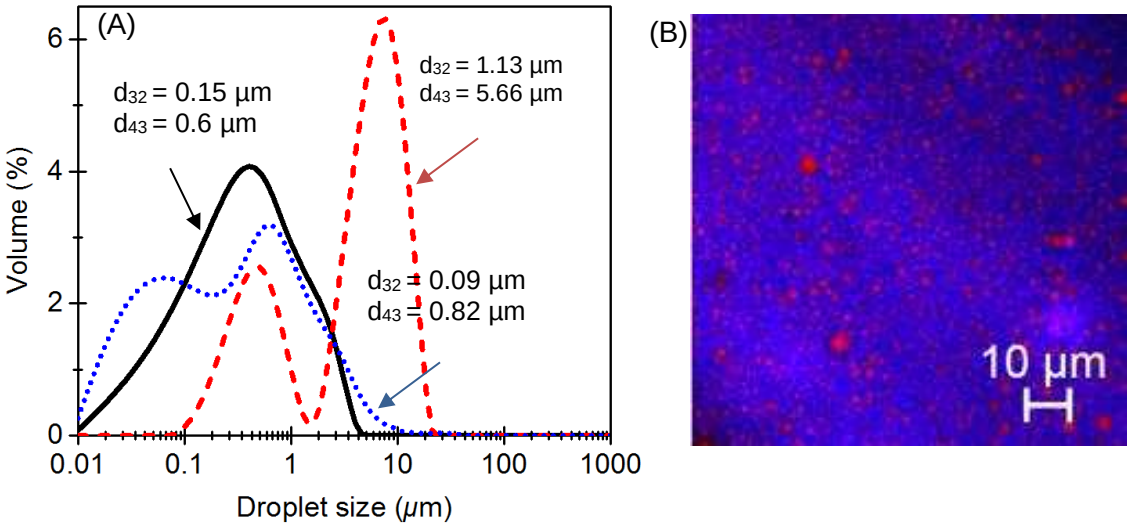


Figure 4. Droplet size distribution (A) indicating $d_{32}$ and $d_{43}$ values of 40 wt% oil-in-water emulsion stabilised by 1 wt% OSA (red dashed line), 2 wt% OSA (blue dotted line) and 4 wt% OSA (black full line) and CLSM micrograph (B) of 40 wt% oil-in-water emulsion stabilised by 4 wt% OSA, oil droplets in red stained using Nile Red and OSA starch in blue stained using Methylene Blue. Scale bar represents 10 µm.

Figure 4A shows the oil droplet size distribution of 40 wt% sunflower oil emulsions stabilised by either 1 wt%, 2 wt% or 4 wt% OSA starch. At the low concentration of OSA starch (1 wt%), the droplet size distribution was bimodal and had a large $d_{43}$ value with significant population of oil droplets in the region of 1 – 20 µm suggesting aggregation or coalescence. Increasing the concentration of OSA starch to 2 wt% led to a significant (90%) decrease of the $d_{32}$ and $d_{43}$ values, to 0.09 and 0.82 µm respectively (Figure 4A). The

significantly lower $d_{32}$ value (0.09 µm) might suggest the formation of OSA starch aggregates in the unadsorbed phase. Previous authors have referred to such aggregates of OSA starch molecules as micelles, although the structures formed must be far more complex than conventional surfactant micelles. Krstonošić et al. (2011), Zhu et al. (2013) and Sweedman et al. (2014) reported critical micelle concentrations between 0.41 - 0.88 g $L^{-1}$. Therefore, at 2 wt% OSA starch, the formation of micelles are unlikely. The increased OSA starch concentration (from 1 to 2 wt%) might have allowed a faster adsorption of the OSA starch to the oil droplet. Furthermore, an increase in viscosity of the aqueous phase, due to the increase of OSA starch concentration, would limit any coalescence (as observed with the emulsion stabilised by 1 wt%) post homogenization and thus significantly reduced the oil droplet size (Nilsson and Bergenståhl, 2006).

. Doubling the concentration of OSA starch further to 4 wt% showed a significant increase in the emulsion stability as the oil droplet size distribution became monomodal and symmetrical. The CLSM image (Figure 4B) further confirms that the oil droplets (in red) were uniformly distributed in agreement with the light scattering data (Figure 4A). These results are in accordance with previous studies conducted on the stabilization properties of OSA starch (Sweedman, Tizzotti, Schäfer & Gilbert, 2013; Tesch, Gerhards & Schubert, 2002). Further studies are needed focusing on kinetics of stability of OSA-starch stabilized emulsions. However, we note that most emulsions, if they exhibit the good stability shown here over 24 h, tend to be stable over much longer periods. Based on these results, further experiments were conducted using this optimized formulation (i.e., 40 wt% oil, 4 wt% OSA starch).

### 3.3 Rheological properties of OSA starch-stabilised emulsion gels

The influence of different concentrations of OSA starch-stabilised emulsions on the rheology of the native sheared wheat starch gels was recorded (Figure 5A and B) over the same

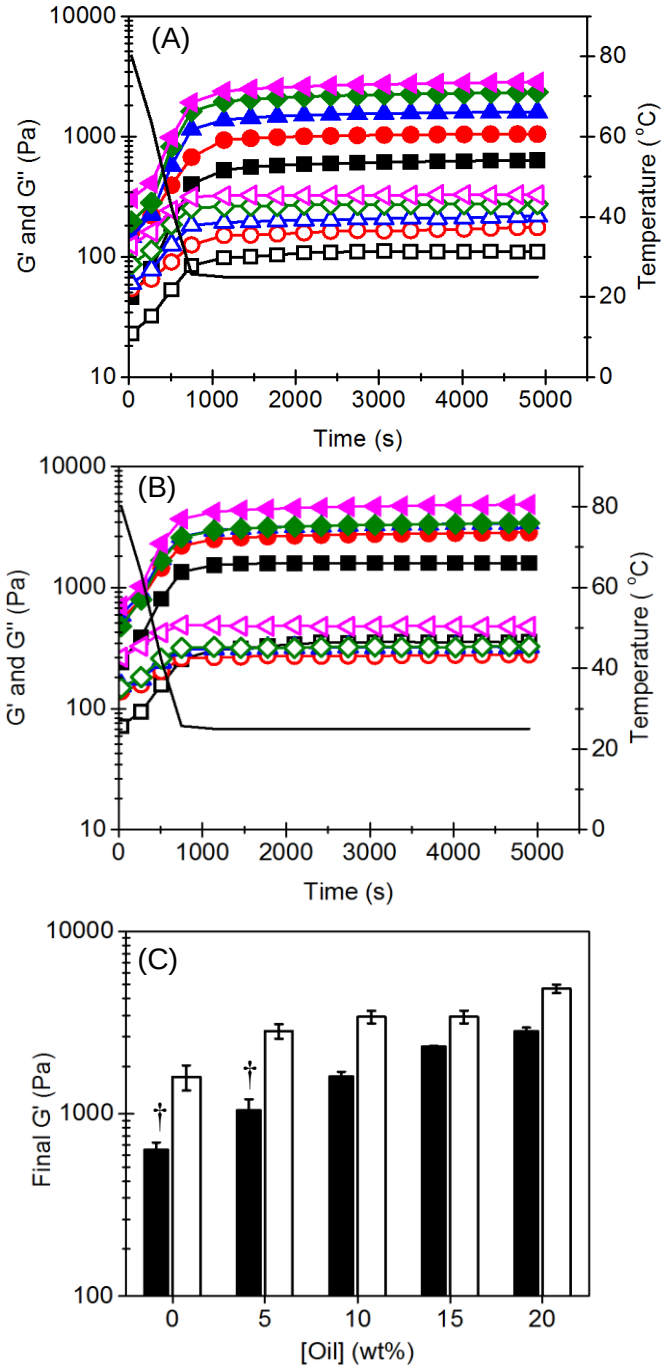


Figure 5. Elastic modulus (G', filled symbols) and viscous modulus (G'', empty symbols) as a function of time and temperature (full line) of 15 wt% native starch gel (A) and 20 wt% native starch gel (B) prepared using different oil fractions (0 wt%, ■; 5 wt%, ●; 10 wt%, ▲; 15 wt%, ♦; 20 wt%, ◄), at 1 Hz and 0.5 % strain. Final elastic modulus of native starch gels at 15 wt% (black) and 20 wt% (white) is shown as a function of oil concentration (C) measured at 25 °C, 1 Hz and 0.5 % strain, samples with symbol (†) are not significantly different ($p > 0.05$) to native starch gel (15 or 20 wt%) without oil droplets.

cooling and holding regime (from 80 to 25 °C followed by 66 min at 25 °C) as discussed for the previous experiments. As in the previous results, all samples showed "gel"-like signature from time 0 s since G' >> G'' and they all had a similar rheological behaviour irrespective of the native starch (15 or 20 wt%) or OSA starch-stabilised emulsion concentrations (5, 10, 15 or 20 wt%).

In contrast with the previous results (samples without added oil droplets) (Figures 2A and 2B), the addition of OSA-stabilised emulsion had a significant impact on the final elastic modulus of the gels (Figures 5A and 5B).The incorporation of the emulsions to 15 wt% native starch gels led to an almost linear increase of the final G' (Figure 5C), although 5 wt% oil appeared to be not sufficient enough to increase the final G' of 15 wt% native starch gel significantly ($p > 0.05$). The addition of 5 wt% emulsion droplets and/or 0.26 wt% OSA starch did not contribute to significant strengthening of the gel matrix, probably because the OSA starch molecules were mainly adsorbed at the surface of the oil droplets and were not in excess to interact with the continuous phase (Dickinson & Chen, 1999). Also, the volume fraction of filler added was not high enough to significantly reinforce the matrix (Torres, Murray & Sarkar, 2016) .

At 20 wt% native starch, the emulsion droplets (5 to 20 wt%) significantly ($p < 0.05$) increased the final G' of the gels (Figure 5B). The addition of 5 to 15 wt% oil provided an average of 50% increase in G', whereas 20 wt% oil strengthened the gel matrix by approximately 70% (Figure 5C). The oil droplet size was on average 0.1 $\mu$m, hence the Laplace pressure means such droplets can be considered effectively as solid particles (van Vliet, 1988). The increase in elastic modulus (G') points to the OSA-starch stabilized emulsion droplets acting as "active fillers" in the starch gel matrix (Dickinson & Chen, 1999; Torres, Murray & Sarkar, 2016, 2017). To our knowledge, this is the first study that reports the use of OSA starch-stabilized droplets as active fillers in starch gels. The binding of the filler (droplets) to the

matrix (native starch gel) was no doubt due to association between the native starch and OSA groups protruding from the surface of the oil droplets. Three types of interactions might have contributed to the filler-matrix association: (i) OSA groups adsorbed at the surface of oil droplets might have some hydrophobic groups oriented towards the aqueous phase allowing the formation of a hydrophobic network between neighbouring OSA groups absorbed on other oil droplets and OSA groups found in the continuous phase; (ii) hydroxyl groups on neighbouring native wheat starch molecules might interact via hydrogen bonding, and (iii) some association between non-absorbed OSA starch molecules (via hydrogen bonding or hydrophobic interaction) may have also made a more minor contribution to the overall modulus – on the basis of the minor effect of OSA starch alone on the native starch gels described above (Bhosale & Singhal, 2007; Singh, Singh, Kaur, Singh Sodhi & Singh Gill, 2003; Sweedman, Tizzotti, Schäfer & Gilbert, 2013).

Similar rheological behaviour has been previously demonstrated using whey protein stabilised emulsion gels (20 wt% oil fraction), where the oil droplets were bound to the matrix via electrostatic, hydrogen bonding and hydrophobic interactions (Dickinson & Chen, 1999; Torres, Murray & Sarkar, 2017). However, no net charges were present in the OSA-stabilised emulsion (data not shown, $\zeta$-potential = 0 ± 0.12 mV), suggesting electrostatic interactions were probably not involved in this case. For comparison purposes, the relative change in final G' was calculated, using $\left|\Delta G'\right| = \left|(G'_{(\text{emulsion gel})} - G'_{(\text{gel})}) / G'_{(\text{emulsion gel})}\right|$, for both whey protein and starch gels at 20 wt% oil. The incorporation of 20 wt% oil droplets with an average size of 0.1 $\mu$m into a whey protein gel matrix led to $\Delta G' \approx 98$ % increase in the strength of the gel (Torres, Murray & Sarkar, 2017), whereas in the starch matrix gel $\Delta G' \approx 67$ %. The absence of strong electrostatic interactions in the starch emulsion gel might explain their significantly weaker elastic modulus as compared to whey protein emulsion gel at the same oil volume

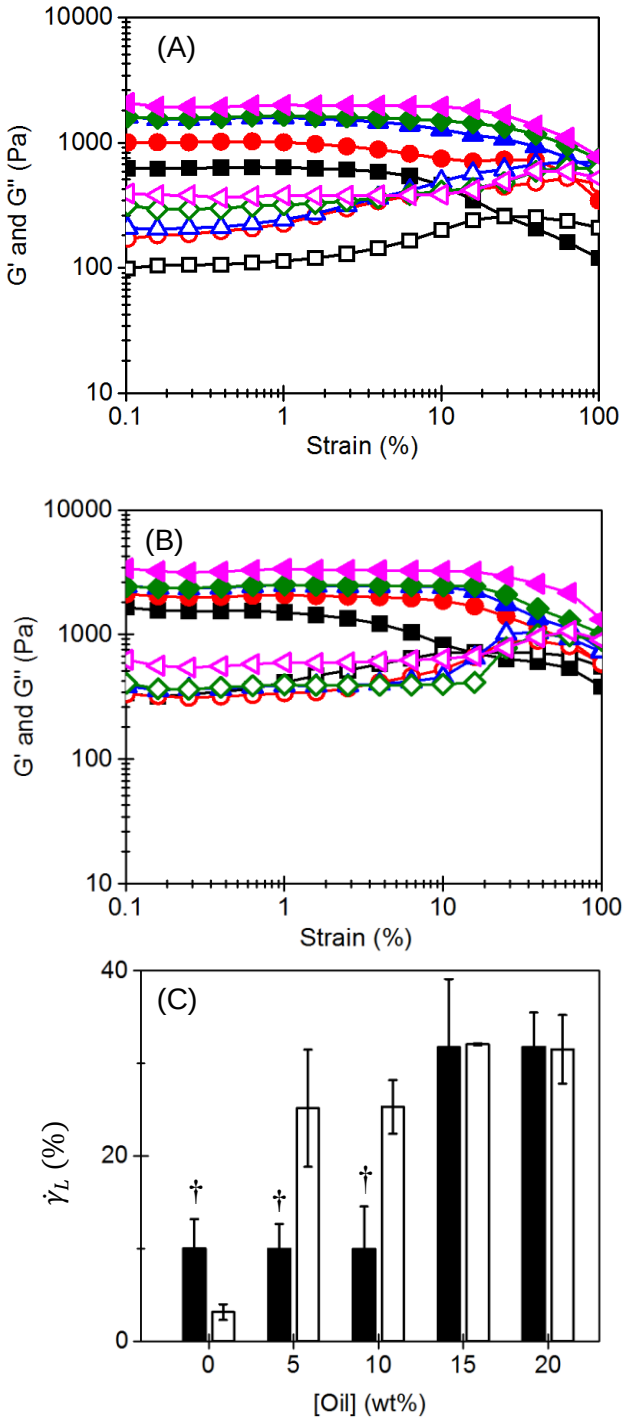


Figure 6. Elastic modulus (G', filled symbols) and viscous modulus (G'', empty symbols) as a function of strain of 15 wt% native starch gel (A) and 20 wt% native starch gel (B) prepared using different oil fractions (0 wt%, ■; 5 wt%, ●; 10 wt%, ▲; 15 wt%, ♦; 20 wt%, ◄). The limiting deformation value ($\dot{\gamma}_L$) of native starch gels at 15 wt% (black) and 20 wt% (white) is reported as a function of oil concentration (C), samples with symbol (†) are not significantly different ($p > 0.05$) to native starch gel (15 or 20 wt%) without oil droplets.

fraction and oil droplet size ($d_{32}$ = 0.1 $\mu$m) (Dickinson, 2012). Under strains 0.1 to 100%, the incorporation of OSA-stabilised oil droplets bound to the native starch gel affected their linear viscoelastic region (LVER), as observed in Figure 6. Low amounts of emulsion (5 and 10 wt%) did not significantly affect the LVER or $\dot{\gamma}_L$of 15 wt% native starch gels, again suggesting that the oil volume fraction or OSA starch concentration was not high enough to significantly interact with the native starch gel matrix. Increasing the oil concentration to 15 and 20 wt% gave a significant increase $\dot{\gamma}_L$ for both gels (Figure 6A and B). For example, $\dot{\gamma}_L$ of 20 wt% native starch gel without emulsion droplets was measured to be 3.2 ± 0.85 % strain, whereas with the addition of 20 wt% oil $\dot{\gamma}_L$ increased to 31.5 ± 3.7 % strain (Figure 6C), i.e. the gels were less brittle. In comparison, whey protein emulsion gel (20 wt% oil fraction) broke down readily at lower $\dot{\gamma}_L$ (6.3 % strain) (Torres, Murray & Sarkar, 2017). Thus, although the filled starch emulsion gels were not as rigid, they may have the rheological advantage of being more flexible.

At the same time, it is seen that the LVER of the emulsion gels with 20 wt% oil was significantly shorter than the LVER of native starch gels with the same freely added OSA starch concentration (2 wt%) (compare Figure 3A and 6A). For example, for 15 wt% native starch gel + 2 wt% of OSA starch, $\dot{\gamma}_L$ of the gel was 79.6 ± 9.43 % strain and 15 wt% native starch gel + 20 wt% emulsion gel $\dot{\gamma}_L$ was 31.8 ± 3.71 % strain (Figure 3A and 6A). In a similar manner, the oil droplets entrapped in the whey protein gel matrices increased the $\dot{\gamma}_L$ from 6.3 to 12.5 % (Torres, Murray & Sarkar, 2017). Thus, oil droplets bound to either whey protein or native starch gel matrices may act as crack initiators weakening the emulsion gel under higher strain.

435 3.4 Characteristics of starch emulsion microgel particles

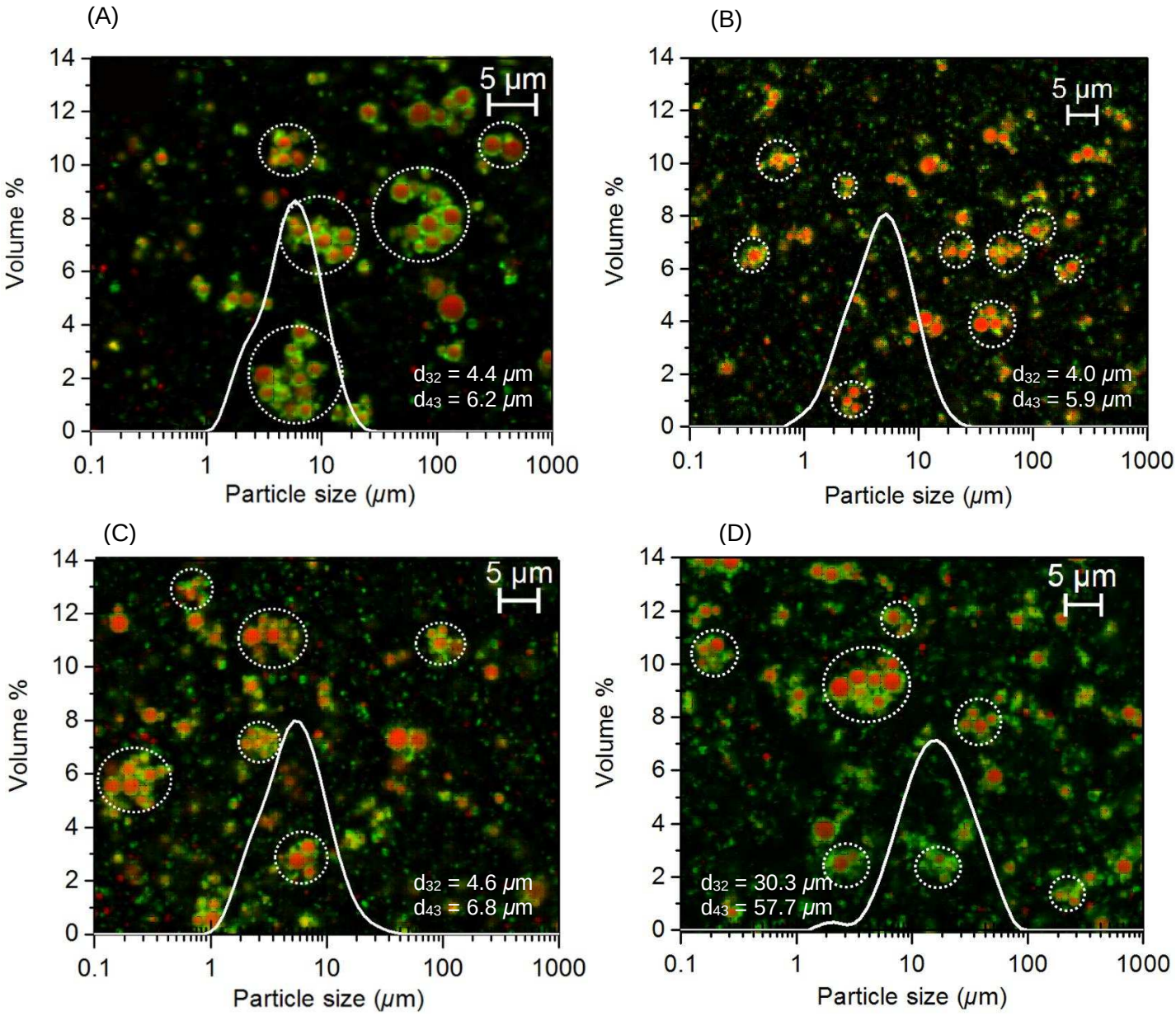


436 Figure 7. CLSM micrograph with superimposed droplet size distribution and $d_{32}$ and $d_{43}$ values
437 of emulsion microgel particles produced at 15 wt% native starch + 5 wt% oil (A), 15 wt%
438 native starch + 10 wt% oil (B), 20 wt% native starch + 10 wt% oil (C) and 20 wt% native starch
439 + 15 wt% oil (D). Dotted circles highlights the emulsion microgel particles in the images.
440 Wheat starch in green, stained with Nile Blue and oil droplets in red stained with Nile Red.

441

442

Starch-based emulsion microgel particles were designed from the emulsion gels with oil fraction (5, 10 and 15 wt%) and the concentration of native wheat starch (15 and 20 wt%) and OSA starch (0.5, 1, 1.5 wt%).

The size of the emulsion microgel particles produced at different concentrations of native starch and oil were similar (Figure 7). At 5-10 wt% oil content, all three particle size distributions were monomodal, (1-10 $\mu$m) with similar $d_{32}$ and $d_{43}$ values (Figure 7A, B and C) (note the $d_{32}$ of encapsulated oil droplets was previously measured as around 0.1 $\mu$m). All the above suggests that the emulsion microgel particle formation process did not lead to significant destabilization and coalescence of the emulsion droplets but that most of the droplets were encapsulated into emulsion microgel particles.

Increasing the oil fraction to 15 wt% led to significantly larger particles with a $d_{32}$ value of 30.3 $\mu$m (Figure 7D). As discussed previously, increasing the oil fraction to 15 wt%, significantly increased the critical strain of the emulsion gel (see Figure 6C). The larger critical strain of the emulsion gel might have allowed the emulsion gel to deform more extensively under high pressure homogenization and fracture the gel into larger particles as compared to emulsion gels with a lower critical strain, which were more brittle and therefore might break down more randomly into smaller emulsion microgel particles (Dickinson, 2012; Moakes, Sullo & Norton, 2015; Torres, Murray & Sarkar, 2017). The emulsion microgel particle morphology was mostly spherical (see Figure 7). No significant variation in morphology was observed at the different concentrations of starch or percentage oil droplets. Most oil droplets (in red) seemed to be entrapped in a starch gel matrix (in green) and no free surface oil was observed after homogenization, suggesting little loss of droplets to the aqueous phase. However, increasing the concentration of starch from 15 to 20 wt% led to a higher amount of matrix debris in dispersion as well as more structures where individual oil droplets (in red) were visibly surrounded by a thin layer of

starch (in green in Figure 7C and D). At higher concentrations of native starch (20 wt%) and oil fraction (10-15 wt%), the final G' and critical strain of the emulsion gel was the highest, forming larger emulsion microgel particles (see above). During the first pass through the homogenizer, the higher native starch concentration and oil fraction enabled the formation of large emulsion microgel particles where some were only loosely bound beneath the surface of the microgel particles. The second pass through the homogenizer might have disrupted such particles and released more individual oil droplets surrounded by fragments of the matrix (Dickinson, 2000; Malone & Appelqvist, 2003).

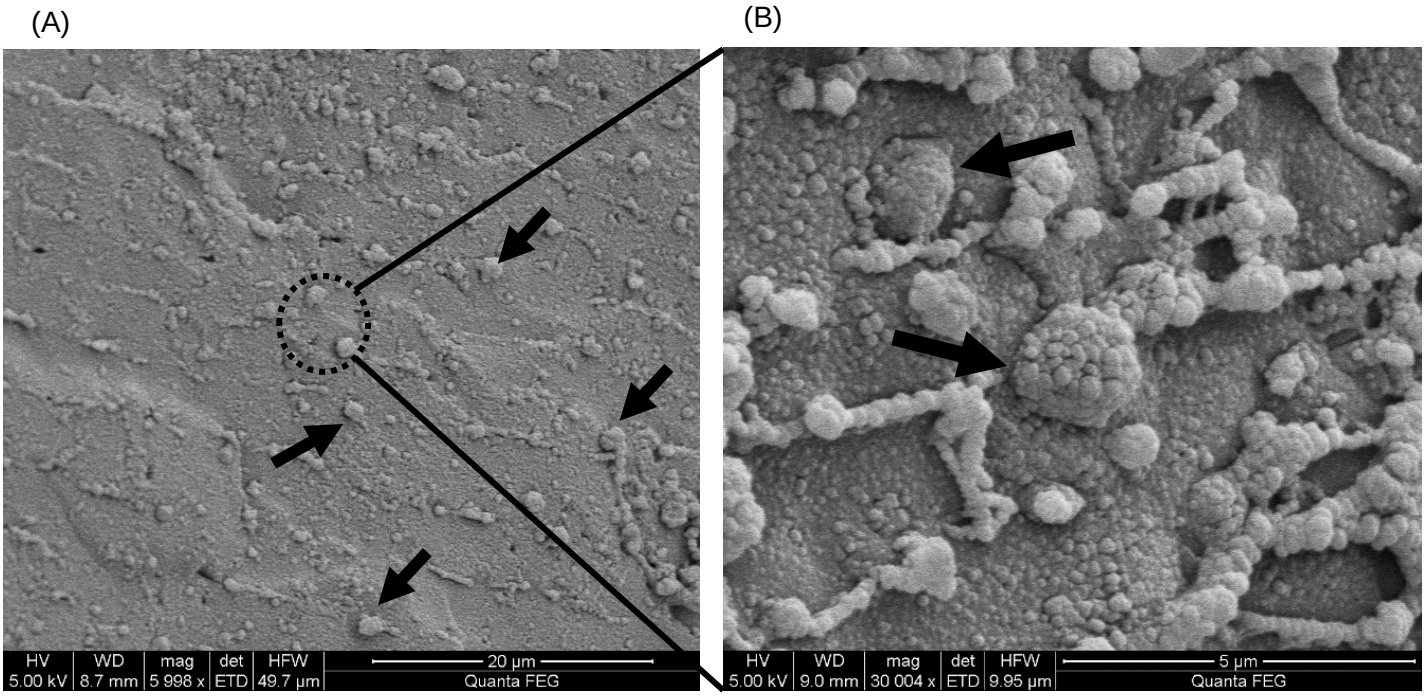


Figure 8**.** Cryo-SEM micrograph of starch emulsion microgel particles produced using 10 wt% OSA-stabilised emulsion encapsulated into 15 wt% native starch, scale bar represents 20 $\mu$m (A) and higher magnification image showing the external surface of the emulsion microgel particles, scale bar represents 5 $\mu$m (B). The arrows point to the individual emulsion microgel particles.

The cryo-SEM micrographs (Figure 8) indicates that emulsion microgel particles were of the order of 2-3 $\mu$m, which is about 40-50% lower as compared to that of CLSM images (Figure 7). This might be due to the potential shrinkage during the cryo-SEM preparation procedure. Figure 8A shows several emulsion microgel particles of similar sizes homogeneously distributed throughout the micrograph. Most particles appeared to be spherical and did not seem to be significantly aggregated. At higher magnification (Figure 8B), a few emulsion microgel particles seemed to have aggregated into linear chains, but this is assumed to be an artefact of the cryo-SEM preparation.

Higher magnification images (Figure 8B) showed that the particles appeared to have a "raspberry-like" surface, which is assumed to be due to the underlying intact encapsulated oil droplets. It has been demonstrated that composite materials containing hydrophobic particles bound to a gel matrix tend to fracture adjacent to the particle surface (Dickinson, 2012; Langley & Green, 1989). Therefore, under shear, one might expect, the emulsion gel to break adjacent to the oil droplet surface, explaining the appearance of the emulsion microgel particle surface.

## 4 Conclusion

Findings from this study have demonstrated that OSA stabilised-emulsion droplets act as active fillers in a sheared native starch gel allowing the design of novel starch emulsion microgel particles i.e., a soft solid network encapsulating several oil droplets into one particle via a facile top-down shearing approach. The emulsion droplets are firmly bound to the gel network, probably due to a combination of three types of associations: the OSA starch at the oil-water interface forming a hydrophobic network with neighbouring OSA starch-stabilized droplets; native wheat starch macromolecules associating together via hydrogen bonding; minor hydrogen bonds forming between hydroxyl groups on OSA starch and native starch in the continuous phase.

Emulsion microgel particles with tuneable sizes and mechanical properties can be produced from starch and OSA starch as long as there is a strong understanding of the interplay between the concentration of the native starch, surface active (OSA) starch, oil volume fraction, gelation kinetics and emulsion gel mechanical behaviour. However, further experiments on these emulsion microgel particles, such as encapsulation efficiency and stability tests over time and temperature are required before such particles can be used in commercial food and personal care application such as, release of lipophilic flavour and aroma molecules.

## 5 Acknowledgments

Author (OT) would like to thank University of Leeds 110 Anniversary scholarship for funding her PhD study. The authors would like to thank Ingredion for providing the commercial OSA starch and Martin Fuller for his technical support in electron microscopy.

## 6 References

Ballauff, M., & Lu, Y. (2007). "Smart" nanoparticles: Preparation, characterization and applications. Polymer, 48(7), 1815-1823.

Bao, J., Xing, J., Phillips, D. L., & Corke, H. (2003). Physical Properties of Octenyl Succinic Anhydride Modified Rice, Wheat, and Potato Starches. Journal of Agricultural and Food Chemistry, 51(8), 2283-2287.

Beaulieu, L., Savoie, L., Paquin, P., & Subirade, M. (2002). Elaboration and characterization of whey protein beads by an emulsification/cold gelation process: application for the protection of retinol. Biomacromolecules, 3(2), 239-248.

Bhosale, R., & Singhal, R. (2007). Effect of octenylsuccinylation on physicochemical and functional properties of waxy maize and amaranth starches. Carbohydrate Polymers, 68(3), 447-456.

533 Dickinson, E. (2000). Structure and Rheology of Simulated Gels Formed from Aggregated
534 Colloidal Particles. Journal of Colloid and Interface Science, 225(1), 2-15.
535 Dickinson, E. (2012). Emulsion gels: The structuring of soft solids with protein-stabilized oil
536 droplets. Food Hydrocolloids, 28(1), 224-241.
537 Dickinson, E., & Chen, J. S. (1999). Heat-Set Whey Protein Emulsion Gels: Role of Active
538 and Inactive Filler Particles. Journal of Dispersion Science and Technology, 20(1-2), 197-213.
539 Kaufman, R. C., Wilson, J. D., Bean, S. R., Herald, T. J., & Shi, Y. C. (2015). Development of
540 a 96-well plate iodine binding assay for amylose content determination. Carbohydrate
541 Polymers, 115, 444-447.
542 Krstonošić, V., Dokić, L., & Milanović, J. (2011). Micellar properties of OSA starch and
543 interaction with xanthan gum in aqueous solution. Food Hydrocolloids, 25(3), 361-367.
544 Langley, K. R., & Green, M. L. (1989). Compression Strength and Fracture Properties of
545 Model Particulate Food Composites in Relation to Their Microstructure and Particle-Matrix
546 Interaction. Journal of Texture Studies, 20(2), 191-207.
547 Lu, T.-J., Duh, C.-S., Lin, J.-H., & Chang, Y.-H. (2008). Effect of granular characteristics on
548 the viscoelastic properties of composites of amylose and waxy starches. Food Hydrocolloids,
549 22(1), 164-173.
550 Malone, M. E., & Appelqvist, I. A. M. (2003). Gelled emulsion particles for the controlled
551 release of lipophilic volatiles during eating. Journal of Controlled Release, 90(2), 227-241.
552 McClements, D. J. (2015). Encapsulation, protection, and release of hydrophilic active
553 components: Potential and limitations of colloidal delivery systems. Advances in Colloid and
554 Interface Science, 219, 27-53.
555 Miles, M. J., Morris, V. J., Orford, P. D., & Ring, S. G. (1985). The roles of amylose and
556 amylopectin in the gelation and retrogradation of starch. Carbohydrate Research, 135(2), 271-
557 281.

558 Moakes, R. J. A., Sullo, A., & Norton, I. T. (2015). Preparation and characterisation of whey
559 protein fluid gels: The effects of shear and thermal history. Food Hydrocolloids, 45, 227-235.
560 Nilsson, L., & Bergenståhl, B. (2006). Adsorption of Hydrophobically Modified Starch at
561 Oil/Water Interfaces during Emulsification. Langmuir, 22(21), 8770-8776.
562 Ortega-Ojeda, F. E., Larsson, H., & Eliasson, A. (2005). Gel formation in mixtures of
563 hydrophobically modified potato and high amylopectin potato starch. Carbohydrate Polymers,
564 59(3), 313-327.
565 Rosalina, I., & Bhattacharya, M. (2002). Dynamic rheological measurements and analysis of
566 starch gels. Carbohydrate Polymers, 48(2), 191-202.
567 Singh, N., Singh, J., Kaur, L., Singh Sodhi, N., & Singh Gill, B. (2003). Morphological, thermal
568 and rheological properties of starches from different botanical sources. Food Chemistry, 81(2),
569 219-231.
570 Svegmark, K., & Hermansson, A.-M. (1991). Changes induced by shear and gel formation in
571 the viscoelastic behaviour of potato, wheat and maize starch dispersions. Carbohydrate
572 Polymers, 15(2), 151-169.
573 Sweedman, M. C., Schäfer, C., & Gilbert, R. G. (2014). Aggregate and emulsion properties of
574 enzymatically-modified octenylsuccinylated waxy starches. Carbohydrate Polymers, 111,
575 918-927.
576 Sweedman, M. C., Tizzotti, M. J., Schäfer, C., & Gilbert, R. G. (2013). Structure and
577 physicochemical properties of octenyl succinic anhydride modified starches: A review.
578 Carbohydrate Polymers, 92(1), 905-920.
579 Tesch, S., Gerhards, C., & Schubert, H. (2002). Stabilization of emulsions by OSA starches.
580 Journal of Food Engineering, 54(2), 167-174.
581 Teyssandier, F., Cassagnau, P., Gérard, J. F., & Mignard, N. (2011). Sol–gel transition and
582 gelatinization kinetics of wheat starch. Carbohydrate Polymers, 83(2), 400-406.

583 Thirathumthavorn, D., & Charoenrein, S. (2006). Thermal and pasting properties of native and
584 acid-treated starches derivatized by 1-octenyl succinic anhydride. Carbohydrate Polymers,
585 66(2), 258-265.
586 Torres, O., Murray, B., & Sarkar, A. (2016). Emulsion microgel particles: Novel encapsulation
587 strategy for lipophilic molecules. Trends in Food Science & Technology, 55, 98-108.
588 Torres, O., Murray, B., & Sarkar, A. (2017). Design of novel emulsion microgel particles of
589 tuneable size. Food Hydrocolloids, 71, 47-59.
590 Tukomane, T., & Varavinit, S. (2008). Influence of Octenyl Succinate Rice Starch on
591 Rheological Properties of Gelatinized Rice Starch before and after Retrogradation. Starch -
592 Stärke, 60(6), 298-304.
593 van Vliet, T. (1988). Rheological properties of filled gels. Influence of filler matrix interaction.
594 Colloid and Polymer Science, 266(6), 518-524.
595 Wang, S., Li, C., Copeland, L., Niu, Q., & Wang, S. (2015). Starch Retrogradation: A
596 Comprehensive Review. Comprehensive Reviews in Food Science and Food Safety, 14(5),
597 568-585.
598 Wei, J., Li, Y., & Ngai, T. (2016). Tailor-made microgel particles: Synthesis and
599 characterization. Colloids and Surfaces A: Physicochemical and Engineering Aspects, 489,
600 122-127.
601 Zhang, N., Liu, H., Yu, L., Liu, X., Zhang, L., Chen, L., & Shanks, R. (2013). Developing
602 gelatin–starch blends for use as capsule materials. Carbohydrate Polymers, 92(1), 455-461.
603 Zhang, Z., Zhang, R., Chen, L., Tong, Q., & McClements, D. J. (2015). Designing hydrogel
604 particles for controlled or targeted release of lipophilic bioactive agents in the gastrointestinal
605 tract. European Polymer Journal, 72, 698-716.
606 Zhu, J., Li, L., Chen, L., & Li, X. (2013). Nano-structure of octenyl succinic anhydride
607 modified starch micelle. Food Hydrocolloids, 32(1), 1-8.

608